A membrane defect in the pathogenesis of the Smith-Lemli-Opitz syndrome

Thomas N. Tulenko,[1,*] Kathy Boeze-Battaglia,[†] R. Preston Mason,[§] G. Stephen Tint,[**] Robert D. Steiner,[††] William E. Connor,[§§] and Edward F. Labelle[***]

Departments of Surgery and Biochemistry & Molecular Pharmacology,* Thomas Jefferson University College of Medicine, Philadelphia, PA; Department of Physiology, School of Veterinary Medicine,*** and Department of Biochemistry, School of Dental Medicine,† University of Pennsylvania, Philadelphia, PA; Elucida Research LLC,§ Beverly, MA, and Brigham and Women's Hospital, Harvard Medical School, Boston, MA; Research Service,** Department of Veterans Affairs Medical Center, East Orange, NJ, and Department of Medicine, University of Medicine and Dentistry of New Jersey Medical School, Newark, NJ; Departments of Pediatrics and Molecular & Medical Genetics,†† Child Development and Rehabilitation Center, Doernbecher Children's Hospital; and Department of Medicine,§§ Oregon Health and Science University, Portland OR

Abstract The Smith-Lemli-Opitz syndrome (SLOS) is an often lethal birth defect resulting from mutations in the gene responsible for the synthesis of the enzyme 3β-hydroxy-steroid-Δ^7-reductase, which catalyzes the reduction of the double bond at carbon 7 on 7-dehydrocholesterol (7-DHC) to form unesterified cholesterol. We hypothesize that the deficiency in cholesterol biosynthesis and subsequent accumulation of 7-DHC in the cell membrane leads to defective composition, organization, dynamics, and function of the cell membrane. Using skin fibroblasts obtained from SLOS patients, we demonstrate that the SLOS membrane has increased 7-DHC and reduced cholesterol content and abnormal membrane fluidity. X-ray diffraction analyses of synthetic membranes prepared to mimic SLOS membranes revealed atypical membrane organization. In addition, calcium permeability is markedly augmented, whereas membrane-bound Na^+/K^+ATPase activity, folate uptake, inositol-1,4,5-trisphosphate signaling, and cell proliferation rates are markedly suppressed. These data indicate that the disturbance in membrane sterol content in SLOS, likely at the level of membrane caveolae, directly contributes to the widespread tissue abnormalities in this disease.—Tulenko, T. N., K. Boeze-Battaglia, R. P. Mason, G. S. Tint, R. D. Steiner, W. E. Connor, and E. F. Labelle. **A membrane defect in the pathogenesis of the Smith-Lemli-Opitz syndrome. *J. Lipid Res.* 2006.** 47: **134–143.**

Supplementary key words 7-dehydrocholesterol • 3β-hydroxy-steroid-Δ^7-reductase • birth defects • cell membrane • caveolae • rafts

The Smith-Lemli-Opitz syndrome (SLOS) was originally described in 1964 by three pediatricians, David Smith, Luc Lemli, and John Opitz (1), who noted the clustering of a variety of abnormalities and malformations in afflicted children. Newborns with SLOS have specific facial abnormalities and often suffer from multiple congenital anomalies, including cleft palate, congenital heart disease, genitourinary abnormalities, and syndactyly. In addition, they typically demonstrate mental retardation and brain abnormalities and are characterized further by an almost uniform failure to thrive (2, 3). Severity varies in SLOS patients, but their parents, although heterozygous, are phenotypically normal. Severity was historically divided into two phenotypes (4): the more severe clinical phenotype was designated type II and was commonly fatal by 6 months of age, whereas the less severe phenotype was designated type I and was compatible with survival into adulthood, albeit with persistence of the clinical features of SLOS (5). More recently, however, phenotypic variations in SLOS have been thought to reflect a continuum (6), because patients with different severities have been shown to have mutations in the same gene (7–9). Based on clinical criteria, the incidence of SLOS was previously suggested to range from 1:20,000 to 1:60,000 (10, 11). However, a more recent study screening for the most common mutation (IV8-1G>C) calculates the carrier frequency for all mutations at 1 in 30, yielding an incidence estimate of 1:1,590 to 1:13,500 (12). A similar frequency was obtained by Nowaczyk et al. (13). By comparison, the three most common autosomal recessive genetic conditions in childhood are commonly listed as cystic fibrosis (1:2,500), phenylketonuria (1:14,000), and galactosemia (1:40,000) (14). Therefore, although not a common disease, SLOS is the second most serious recessive genetic condition.

Originally, SLOS was defined and diagnosed solely by clinical criteria. However, Irons, Tint, and colleagues (15,

Manuscript received 18 July 2005 and in revised form 25 October 2005.

Published, JLR Papers in Press, October 28, 2005.
DOI 10.1194/jlr.M500306-JLR200

[1] To whom correspondence should be addressed.
e-mail: thomas.tulenko@jefferson.edu

16) were the first to show that increased blood levels of 7-dehydrocholesterol (7-DHC) occurred in SLOS patients, a finding that ultimately led to the discovery of specific mutations in the enzyme that catalyzes the biosynthesis of cholesterol, 3β-hydroxy-steroid-Δ^7-reductase (DHCR7) (7–9). SLOS is now diagnosed by increased blood levels of the immediate precursor to cholesterol synthesis, 7-DHC, coupled with low cholesterol levels. Moreover, the clinical severity of SLOS has also been shown to correlate with the levels of blood 7-DHC and cholesterol (17, 18), although the correlation between sterol levels and clinical severity is not always strong. Additional evidence supporting a defect in DHCR7 enzyme activity as the biochemical basis for clinical features of SLOS is found in the early (19) and more recent work (20) from Roux's group demonstrating that inhibitors of DHCR7 (AY 9944 and BM 15.766) produce teratogenic malformations and sterol abnormalities in rats similar to those seen in humans. Xu et al. (21) have confirmed these findings with BM 15.766, and Honda et al. (22) have extended these observations to human skin fibroblasts, in which BM 15.766 inhibited DHCR7 enzyme activity and resulted in the accumulation of 7-DHC and the depletion of cholesterol, thereby inducing SLOS at the cellular level. Because cholesterol is absolutely required for the biosynthesis of cell membranes, steroids, and sex hormones, the altered sterol synthesis in SLOS patients may underlie the widespread tissue and organ malformations.

Because the genetic defect in SLOS leads to a decrease in cholesterol and a concomitant increase in 7-DHC, it is reasonable to consider that this sterol imbalance may contribute to SLOS pathogenicity. On first glance, the similarities between cholesterol and 7-DHC appear to dominate (i.e., they differ by only a double bond between the 7 and 8 carbons in 7-DHC) (**Fig. 1**). Accordingly, this minor structural difference may not be biologically relevant. In fact, an example of this was shown by Cooper et al. (23), who found that 7-DHC can replace cholesterol in its activation of the sonic hedge-hog protein (*Shh*) without loss of function, suggesting that the pathogenic defect in SLOS is not at the level of early embryonic segmentation mediated by *Shh*. However, the absolute requirement for cholesterol in the synthesis and function of cell membranes raises the question of whether decreased cholesterol, increased 7-DHC, or their combination might cause abnormalities in membrane function. Moreover, unique cholesterol-rich domains (i.e., rafts and caveolae in the cell membrane) participate in membrane transport and signaling in a wide variety of cells, and the degree to which their function is altered by these SLOS sterol alterations has not been established.

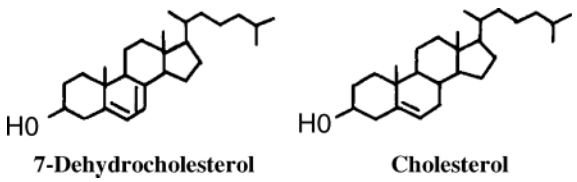

Fig. 1. Similarity of molecular structures of 7-dehydrocholesterol (7-DHC) and cholesterol. Note that the only difference is the double bond between carbons 7 and 8 in 7-DHC.

In this study, we used skin fibroblasts obtained from SLOS patients to evaluate whether membrane sterol composition, organization, and dynamics are abnormal. We found that membrane lipid dynamics were altered in SLOS cells. Moreover, they were accompanied by alterations in membrane calcium permeability, Na^+/K^+ATPase activity, folate uptake, inositol-1,4,5-trisphosphate (IP_3) signaling, and cell proliferation, suggesting altered membrane function by the SLOS sterol alterations. Together, these findings demonstrate that in SLOS patients, the accumulation of 7-DHC, and/or the deficiency in cholesterol biosynthesis, results in cell membranes that are defective and likely contributes to the cellular pathobiology in SLOS patients.

METHODS

Skin fibroblasts were obtained from patients with SLOS and healthy control subjects and grown to confluence in MEM + 10% FBS supplemented with nonessential amino acids. Before the experiments, the SLOS cells were transferred to MEM + 10% lipoprotein-deficient serum (LPDS) for 5–7 days to remove exposure to exogenous cholesterol (lipoproteins) otherwise present in normal FBS. Fibroblasts from five SLOS patients and five control subjects were used. The ages of the controls were 2, 2, 7, 9, and 12 years, and the ages of the SLOS patients were 3 months and 4, 9, 12, and 12 years. All cells were studied between passage two and eight, and all assays were performed at 37°C. Approval to use human skin fibroblasts before the initiation of this study was granted by the University Institutional Review Board.

For membrane sterol measurements, intact microsomes enriched with plasma membranes were isolated as described previously (24, 25). After the addition of 1 mg of coprostanol as an internal recovery standard, membrane pellets were extracted in chloroform-methanol (26). The chloroform phase was obtained and dried under nitrogen. Sterols were identified and quantitated using GC-MS as described previously (16). Briefly, an aliquot of the extract was hydrolyzed in 1 N NaOH ethanol for 1 h at 70°C, extracted with *n*-hexane, and converted into trimethylsilyl ether derivatives followed by injection into a capillary column. This column was a chemically bonded, fused silica, nonpolar CP-Sil 5CB (25 m × 0.25 mm inner diameter; stationary phase, 100% dimethylsiloxane) (Chrompack, Raritan, NJ), and helium was used as the carrier gas at a flow rate of 1 ml/min. To achieve optimal separation of sterols, the column oven temperature was programmed to change from 100°C to 265°C at 35°C/min after a 2 min delay from the time of injection. The chromatograph was calibrated with a calibration standard consisting of 1 μg each of authentic coprostanol and 7- and 8-DHC (Supelco). Membrane sterol content is expressed as sterol-protein ratios. Protein determinations were performed using the method of Lowry et al. (27).

For membrane fluidity, steady-state anisotropy (1/membrane fluidity) was measured as described previously (28, 29). *cis*-Parinaric acid (CPA) was introduced into membrane vesicles by incubation of a membrane suspension (5.0 ml) with CPA such that the final concentration was 0.5 mol% relative to fibroblast phospholipid for 15 min at 37°C. Fluorescence measurements were made with excitation at 300 nm and emission at 410 nm using a Perkin-Elmer LS50B spectrofluorimeter equipped with

automatic polarizers. All fluorescence values were corrected for scattering and background fluorescence by subtraction of the values obtained from unlabeled membrane suspensions. Steady-state fluorescence anisotropy (r_{ss}) was calculated using the modified Perrin equation (30):

$$r_{ss} = I_{VV} - GI_{VH}/I_{VV} + 2GI_{VH}$$

where G is calculated as $G = I_{HV}/I_{HH}$ and I_{VH} and I_{HH} equal fluorescence intensities perpendicular and parallel, respectively, to the excitation plane.

Membrane structure was probed using a small-angle X-ray diffraction technique as described previously (24, 25). This highly quantitative technique enables the measurement of membrane structure and organization. Briefly, synthetic membranes were prepared (25) [cholesterol, 7-DHC, and dimyristoylphosphatidylcholine (PC), 1:1:2] and sedimented by centrifugation (35,000 *g* for 1 h at 5°C). On completion of the spin, the pelleted membranes were mounted on a curved glass support such that the plane of the bilayer was parallel to the incident X-ray beam. X-ray diffraction was collected using a collimated, monochromatic copper K_α X-ray source that was focused on the sample at near grazing incidence in a temperature- and humidity-controlled brass canister. Diffraction data from the oriented membrane multilayer samples were recorded on a one-dimensional position-sensitive electronic detector (Innovative Technologies, Inc., Newburyport, MA). In addition to direct calibration of the detector system, cholesterol monohydrate was used to verify the calibration. The X-ray reflections collected on film were integrated using a densitometer, whereas the data from the electron detector were analyzed directly using a standard integration algorithm. One-dimensional electron density profiles generated by Fourier analysis of the diffraction data were used to characterize the distribution of the lipid constituents at a resolution of 5–10 Å.

Calcium permeability measurements were made as described previously (28). Briefly, nearly confluent cells on six-well plates were equilibrated in PBS for 60 min before experiments were begun. For assay, PBS was aspirated and replaced with $^{45}Ca^{2+}$-PBS (4 μCi/ml), and the cultures were incubated with $^{45}Ca^{2+}$ for 45 s. $^{45}Ca^{2+}$ uptake was terminated by placing the dishes on a −6°C frosted cradle, followed by immediate, rapid washing of the cells with eight washes of 2 ml of ice-cold (0–2°C) PBS (5 s per wash). Preliminary experiments demonstrated that this wash protocol removed extracellular $^{45}Ca^{2+}$ while retaining intracellular $^{45}Ca^{2+}$ and was equally effective in normal and SLOS cells. The cells were then lysed with SDS (1 mg/ml), and aliquots of the lysate were analyzed for protein content and radioactivity. Calcium uptake was determined from counts derived from the cell lysate $^{45}Ca^{2+}$ fraction (cpm) divided by the specific activity of the $^{45}Ca^{2+}$-containing uptake medium (cpm/μmol Ca^{2+}). The unidirectional inward flux of calcium was measured by exposing cells to $^{45}Ca^{2+}$-PBS for 45 s and is expressed as nanomoles of Ca uptake per milligram of protein per minute. Preliminary experiments demonstrated that his incubation time falls within the linear portion of the calcium uptake curve.

Steady-state Na^+/K^+ATPase activity in control and SLOS fibroblasts grown to confluence was measured as described previously (31) with modifications for cultured cells. Activity was assessed using a 20 min pulse of the kaliometic isotope ^{86}Rb (1 μCi/ml) in the presence and absence of ouabain (3 mM), followed by rapid washing with PBS. The cells were digested in 1% SDS, and the digest was counted for radioactivity using a liquid scintillation counter. Ouabain-insensitive ^{86}Rb uptake was subtracted from total ^{86}Rb uptake to obtain ouabain-sensitive Na^+/K^+ATPase activity, which is expressed as nanomoles of Rb per milligram of cell protein per minute.

For folate uptake measurements, uptake of the reduced folate derivative 5-methyltetrahydrofolate into the cytosol of fibroblasts was quantitated using the method described by Stevens and Tang (32). Briefly, cells were incubated with 5 nM 5-[^{3}H]methyltetrahydrofolate (0.5 μCi) in folate-free medium for 15, 30, 45, and 60 min at 37°C. The medium was removed and the cells were washed four times with PBS followed by the addition of 1.5 ml of lysis buffer (10 mM Tris-HCl, pH 8.0, 20 μg/ml leupeptin, 20 μg/ml aprotinin, and 1 μM 5-methyltetrahydrofolate) to each well. The cells were then lysed by placing the culture plates at −80°C for at least 15 min and thawed on ice. The cells were collected and centrifuged for 20 min at 100,000 *g* in a Beckman ultracentrifuge to separate the membrane pellet from the cytosolic (supernatant) fractions. The radioactivity in each fraction was quantitated by scintillation counting. Nonspecific uptake was measured using 2.5 μM 5-[^{3}H]methyltetrahydrofolate and subtracted from the total radioactivity to give the specific uptake. The results were normalized to total cell protein determined using the method of Lowry et al. (27).

Inositol phosphate (IP) production in SLOS fibroblasts was determined by the procedure of Carney et al. (33). Confluent monolayers of SLOS fibroblasts were prepared in T75 culture flasks, and [^{3}H]inositol (2 μCi/ml) was added to each flask and allowed to incubate for 36 h. The reaction was stopped by rinsing the plates in ice-cold phosphate-buffered saline and adding 2 ml of trichloroacetic acid (10%) to each plate. After 5 min, the TCA was removed and the plate was rinsed with an additional 2 ml of TCA. The combined TCA washes were extracted five times with ethyl ether to remove the TCA, and the aqueous phase was applied to 1 ml Dowex (1 × 8–50 resin formate form, 200–400 mesh) columns. The columns were eluted with water to remove free inositol, followed by 0.1 M formic acid containing 0.2 M ammonium formate to remove [^{3}H]inositol-4-phosphate (IP_1), 0.4 M ammonium formate to remove [^{3}H]inositol-1,4-bisphosphate (IP_2), and 1 M ammonium formate to remove [^{3}H]IP_3. The radioactivity of each fraction was determined by liquid scintillation counting. Total IPs were derived by adding the counts from the IP_1, IP_2, and IP_3 fractions.

Cell proliferation was assessed by measuring [^{3}H]thymidine uptake into DNA as described previously (34). Cells were grown to near confluence and incubated overnight with [^{3}H]thymidine. The cells were then rinsed with PBS followed by extraction and rinsing five times with 10% TCA. The TCA-precipitable material was dissolved overnight with 0.5 ml of KOH (0.5 M) at 23°C, followed by treatment with 0.25 ml of HCl (1 M) before being transferred to scintillation vials (10 ml volume), and the radioactivity was determined by liquid scintillation counting.

Enrichment of the SLOS cell membranes with cholesterol was accomplished using cholesterol-rich liposomes as described previously (28, 34). Cholesterol-rich liposomes were prepared by cosonication of cholesterol with egg phosphatidylcholine in a 2:1 molar ratio, followed by centrifugation, filter sterilization, and confirmation by gas-liquid chromatography and phospholipid-phosphorus colorimetry before experimentation. Cell monolayers were incubated with cholesterol-donor liposomes (250 μg liposomal cholesterol/ml) and incubated for 24 h at 37°C. At the end of the incubation, the cells were washed with PBS containing 0.1% BSA to remove any adherent liposomal particles from the cell surface membranes. Wells from each experiment were assayed for cholesterol content to verify enrichment.

In all experiments, n equals the number of patients studied, and the data are expressed as the mean ± SEM. In most experiments, statistical analysis was performed on paired and unpaired data by use of Students *t*-test or repeated-measures ANOVA. Multiple comparisons were analyzed using the Newman-Keuls test. Statistical significance was taken as $P < 0.05$.

RESULTS

SLOS fibroblasts grown in medium containing 10% FBS show normal cholesterol and modest 7-DHC content (28.0 ± 7.43 and 1.07 ± 0.44 μg/mg protein, respectively) compared with cells maintained on delipidated serum (10% LPDS) for up to 1 week (32.36 ± 1.47 and 7.13 ± 1.46 μg/mg protein, respectively). These values of cholesterol and 7-DHC in SLOS cells are in close agreement with those reported by Wassif et al. (9) in SLOS fibroblast also grown in LPDS. LPDS removes the source of exogenous cholesterol (from lipoprotein) and results in the development of membrane sterol profiles typical of SLOS (**Fig. 2**). Because normal activity of DHCR7 is present in control cells, the primary sterol typically found in normal fibroblasts is cholesterol, with only negligible levels of 7-DHC. The presence of accumulated 7-DHC and reduced levels of cholesterol in their membranes confirms impaired DHCR7 activity in the SLOS cells in this study. Although 8-DHC is also present in the blood of SLOS patients, its conversion from 7-DHC occurs primarily in the liver (35). For this reason, increased 8-DHC levels would not be expected in fibroblasts serially passed in culture. The low 8-DHC levels (0.33 ± 0.03 μg/mg protein) detected in the SLOS cells likely reflect a small degree of cellular conversion of 7-DHC to 8-DHC. That impaired DHCR7 is the sole reason for the appearance of DHCs in SLOS fibroblasts is supported by the observation that the total sterol content in the SLOS membrane is not significantly different between control and SLOS cells. It is important to note, however, that measurements in cultured cells may not be in complete agreement with similar assessments made in vivo, but because of limitations in obtaining enough freshly purified fibroblasts from young children, in vivo studies were not possible in this study.

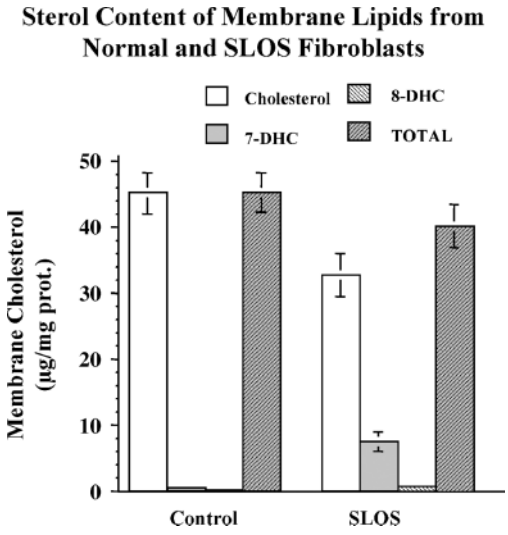

Fig. 2. Sterol composition of normal (left) and Smith-Lemli-Opitz syndrome (SLOS; right) cell membranes. Cells were grown to near confluence in MEM + 10% FBS, followed by incubation in MEM + 10% lipoprotein-deficient serum for 7–10 days (n = 5 subject cell lines/group). Error bars represent mean ± SEM.

To assess the physical state of the cell membrane in SLOS cells, we used two independent experimental strategies. In the first, we assessed membrane fluidity by measuring fluorescence anisotropy, a property inversely related to membrane fluidity. The fluorophore used in this study was CPA, a fluorescent sterol probe that reports on fluidity in the hydrocarbon core (fatty acyl chain region) of the membrane (36). As illustrated in **Fig. 3A**, anisotropy was reduced in the membranes isolated from SLOS cells, reflecting a significant increase (~20%) in membrane fluidity in the fatty acyl region of the membrane. Supporting this finding was a decrease in electron density in this region observed using the second strategy, small-angle X-ray diffraction (Fig. 3B). In this experiment, diffraction was obtained using synthetic membranes prepared to resemble the SLOS membrane (i.e., ~25% of the

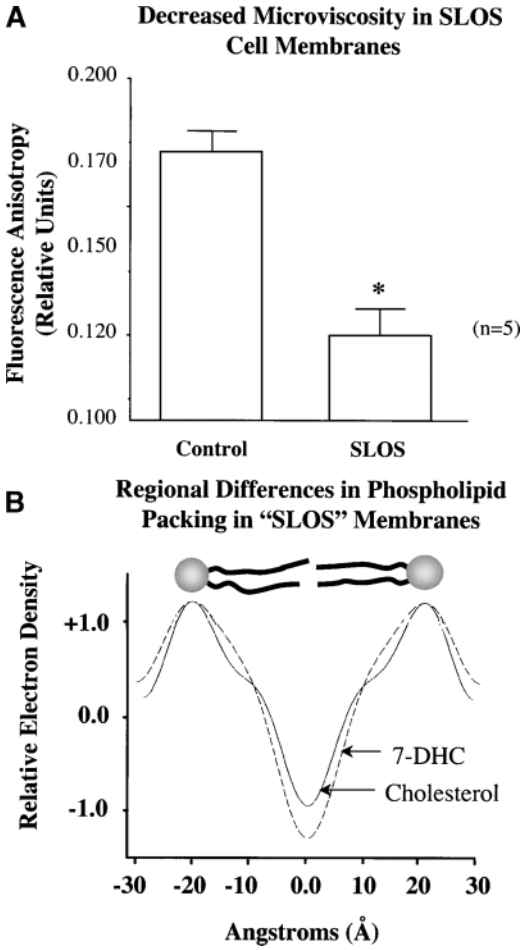

Fig. 3. A: Increased membrane fluidity (decreased anisotropy) in plasma membranes of SLOS fibroblasts. The probe used in this study was *cis*-parinaric acid. * $P < 0.05$; n = 5 subject cell lines/group. B: X-ray diffraction analysis in model membranes prepared with sterol-phospholipid ratios observed in control fibroblasts (solid line) and SLOS fibroblasts (broken line). Note the increase in electron density seen at the membrane surface and the decreased electron density seen in the hydrocarbon core region in the SLOS versus control membranes, reflecting an increase and decrease, respectively, in phospholipid packing in these regions. A model phospholipid bilayer is shown at the top of the electron density profile for orientation. Error bars represent mean ± SEM.

total lipid was 7-DHC). Thus, both approaches to assess the membrane physical state indicate reduced molecular packing in the fatty acyl chain region of the membrane bilayer. Interestingly, the electron density at the surface of the membrane obtained from the X-ray data appeared to be increased, reflecting an increase in molecular packing at the surface of the membrane.

Having established that the physical state of the membrane is disturbed in SLOS cells, we then assessed membrane functional properties. Using ^{45}Ca, unidirectional calcium uptake was observed to be increased by 3-fold in SLOS cells compared with control cells (**Fig. 4**). Adding cholesterol back to the cells decreased calcium permeability approximately halfway back toward control levels. Using the kaliometic isotope $^{86}Rb^{+}$ to follow K^{+}, we observed a marked decrease in ouabain-sensitive Rb uptake in the SLOS cells (**Fig. 5**). This technique has been shown by us and others to directly measure membrane-bound Na/K ATPase activity (31, 37). Like calcium permeability, Na/K ATPase activity also returned about halfway toward control levels after enrichment with exogenous cholesterol. Enrichment of the SLOS cells with cholesterol increased cholesterol content by 42.4% (29.5 ± 5 vs. 42.0 ± 7 μg/mg protein), with no change in 7-DHC content.

A significant anatomic malformation found in many SLOS patients is cleft palate. Because cleft palate has been established to result, in part, from folate deficiency, we assessed folate uptake in the SLOS cells. As illustrated in **Fig. 6**, folate uptake, using a [^{3}H]methyltetrahydrofolate protocol, was suppressed by ~50% in the SLOS cells.

Cell signaling by IP occurs by enzymatic cleavage of inositol from membrane-resident phosphatidylinositol. To determine whether membrane-mediated IP signaling is altered in SLOS, we measured IP production in control and SLOS fibroblasts. A decrease of ~50% was observed among all the IPs: IP_1, IP_2, IP_3, and total IPs (**Fig. 7A**). The reduction was statistically significant among all of the IPs with the exception of IP_3, which approached (P=0.06) but did not reach statistical significance. The reduction in IPs in SLOS cells does not reflect a reduction in the cellular inositol lipid pools, because labeling to isotopic equilibrium demonstrated equivalent labeling in both control and SLOS cells (Fig. 7B). These data reflect general impairment in membrane-mediated cell signaling through the IP pathway in SLOS cells.

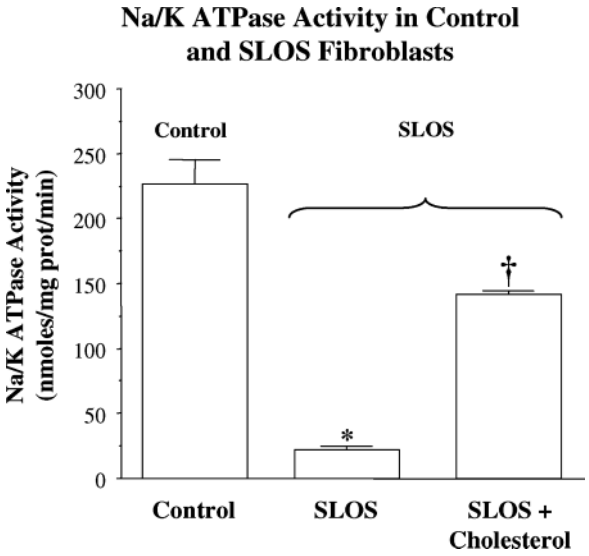

Fig. 5. Steady-state Na^{+}/K^{+}ATPase in control and SLOS fibroblasts. Cholesterol enrichment restores Na^{+}/K^{+}ATPase activity toward control levels in SLOS fibroblasts. The data represent triplicate measures in cell lines from each of three control subjects and three SLOS patients. * $P < 0.001$, SLOS versus control; † $P < 0.01$, SLOS + cholesterol versus SLOS. Error bars represent mean ± SEM.

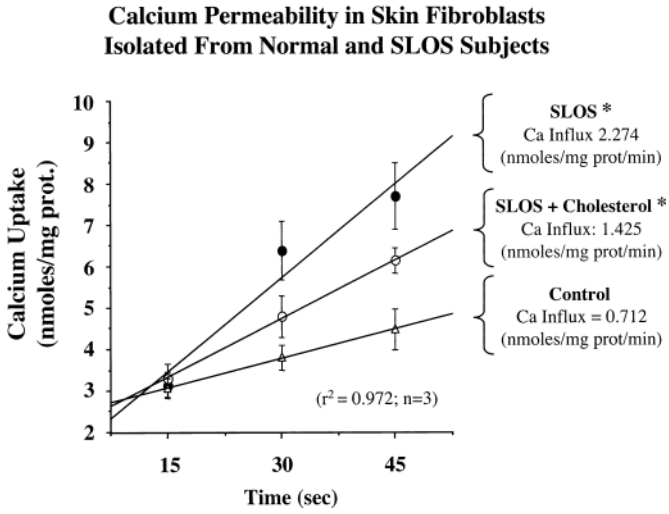

Fig. 4. Increase (three times) in calcium permeability in SLOS versus control fibroblasts. Cholesterol enrichment restores calcium permeability toward control levels in SLOS fibroblasts. The data represent triplicate measures in cell lines from each of three control subjects and three SLOS subjects. * $P < 0.01$, versus control. Error bars represent mean ± SEM.

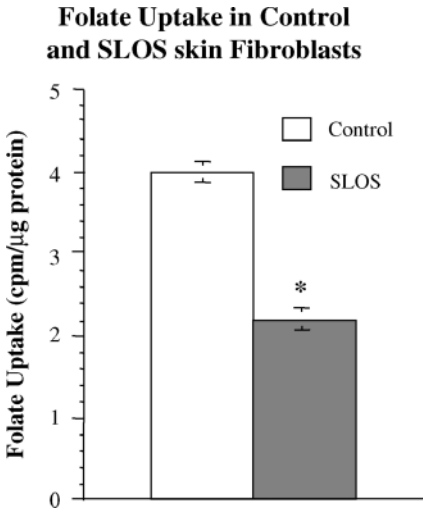

Fig. 6. Reduced folate uptake in SLOS fibroblasts compared with control fibroblasts. The data represent triplicate measurements from two SLOS patients and two control subjects. * $P < 0.01$. Error bars represent mean ± SEM.

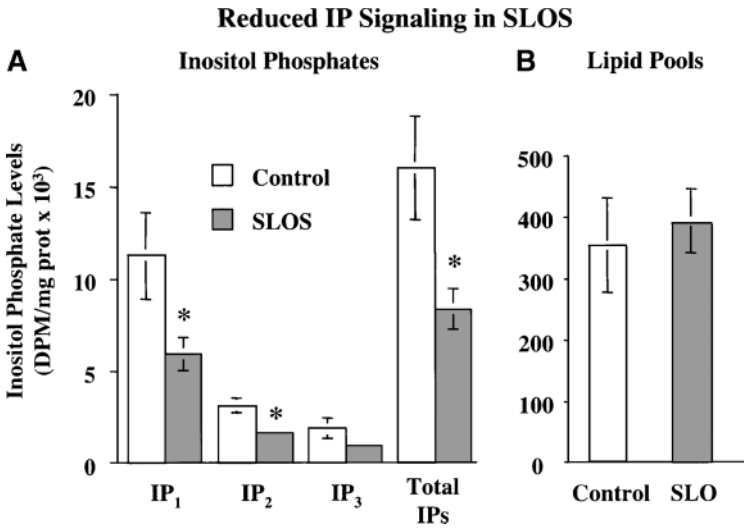

Fig. 7. A: Reduced inositol phosphate (IP), inositol-1,4-bisphosphate (IP_2), inositol-1,4,5-trisphosphate (IP_3), and total IP generation and its recovery after cholesterol enrichment in SLOS fibroblasts compared with normal fibroblasts. B: Control and SLOS cells were incubated with [^{3}H]inositol (10 μCi/ml) for 24 h followed by lipid extraction and counting of radioactivity by liquid scintillation. The data represent triplicate measures in cell lines from four SLOS patients and five control subjects. * $P < 0.05$. Error bars represent mean ± SEM.

Finally, during the daily care and feeding of the SLOS cells, it became clear that the SLOS cells were growing more slowly than the control cells. For this reason, we measured cell proliferation rates using a [^{3}H]thymidine uptake protocol. As shown in **Fig. 8**, SLOS fibroblasts incorporated thymidine at less than half the rate seen in control fibroblasts, reflecting a reduced rate of cell proliferation. Reduced cell proliferation was confirmed in some experiments by direct cell counting (data not shown).

DISCUSSION

The elucidation of an inherited defect in DHCR7 enzyme activity as the biochemical abnormality underlying SLOS by Irons, Tint, and colleagues (15, 16) has led to the identification of the molecular basis of the SLOS syndrome. Molecular cloning of the human DHCR7 cDNA by Moebius et al. (38) demonstrated that DHCR7 is a membrane-bound protein with a molecular mass of 55 kDa with six to nine transmembrane domains. Chromosomal mapping localized the gene to chromosome 11q12-13. A variety of mutations in the DHCR7 gene have been reported in patients with SLOS, including missense, nonsense, frame shift, and splice site mutations (7–9, 38), and all are associated with reduced blood and tissue cholesterol levels with increases in 7-DHC. Moreover, regardless of the nature of the mutation, the degree of cholesterol synthesis by the mutant DHCR7 determines the ratio of cholesterol to 7-DHC, which is somewhat predictive of the severity of the disease (18).

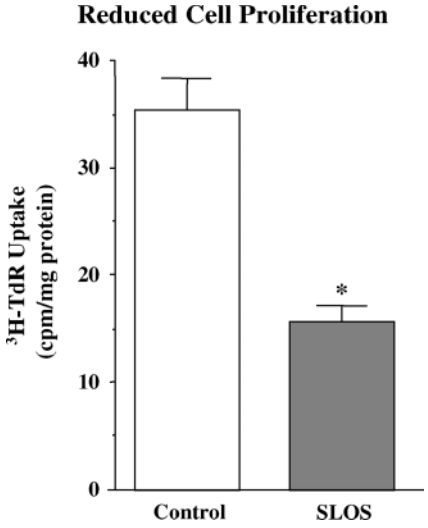

Fig. 8. Reduced cell proliferation in SLOS fibroblasts. Cells were plated on six-well plates, grown to near confluence, and incubated overnight with [^{3}H]thymidine (^{3}H-TdR). Radioactivity was measured in the TCA-insoluble (DNA) fraction. The data represent triplicate measures in fibroblasts from five SLOS patients and five control subjects. * $P < 0.01$. Error bars represent mean ± SEM.

Although the genetic basis of SLOS and the resulting depletion of cholesterol and accumulation of 7-DHC in tissues have been demonstrated, the cellular defects associated with SLOS have not been well described. Accordingly, we analyzed a variety of membrane functions in fibroblasts obtained from SLOS patients to test the hypothesis that a defect exists in the lipid bilayer of SLOS cells that alters the membrane in ways that interfere with the function of various membrane proteins, and thus also cell and tissue function, in this disease. We surmise that such a defect would be caused by the presence of 7-DHC, reduction in cholesterol, or a combination of the two. That the cell's plasma membrane is altered in this disease is confirmed on the basis of a relative depletion of cholesterol (27.8%) and a massive accumulation of 7-DHC (~264-fold) in the membranes of fibroblasts isolated from SLOS patients (Fig. 2). As anticipated, 7-DHC content was exceedingly low (0.027 ± 0.009 μg/mg protein) in membranes isolated from fibroblasts obtained from normal subjects. Interestingly, the total sterol content of SLOS membranes was not significantly different from that of normal membranes. Despite their similar total sterol content, membrane fluidity was increased significantly

(~20%) in membranes isolated from SLOS patients (Fig. 3A). The fluorophore used to evaluate fluidity, CPA, reports on molecular packing in the center (i.e., the fatty acyl chain region of the membrane). This observation is confirmed in X-ray diffraction data obtained from model membranes prepared from cholesterol, 7-DHC, and PC to mimic the SLOS membrane. As shown in Fig. 3B, the relative electron density is decreased in the fatty acyl chain region of the membrane, confirming the decreased intermolecular packing of phospholipid fatty acyl chains suggested by the fluorescence anisotropy data. This decrease in acyl chain packing is associated with a reciprocal increase in molecular packing at the surface of the membrane. A reciprocal relationship between core and surface molecular packing density of the membrane has been established by others as a typical feature in a variety of membranes (39, 40). These data using two separate, different, and independent methods to assess molecular packing in the membrane (i.e., fluidity and X-ray diffraction) clearly demonstrate that the apparently minor differences between cholesterol and 7-DHC structure confer significant differences in membrane lipid organization and dynamics. Although tissue sterols in SLOS have been reported (22), this is the first report of membrane sterol composition, dynamics, and organization in this disease.

To determine whether these are associated with alterations in membrane function, we assessed two key membrane properties that have been widely established as fundamentally important to cell biology across the phylogenetic spectrum: membrane calcium permeability and membrane-bound Na^+/K^+ATPase activity. As shown in Fig. 4, calcium permeability is increased by 3-fold in SLOS fibroblasts compared with controls. The identity of this altered calcium entry pathway cannot be determined from our data, but it likely involves either nonselective or selective ion channels (i.e., voltage-gated, receptor-gated, capacitative calcium entry channels, etc.). Interestingly, after cholesterol enrichment, the augmented calcium permeability in SLOS cells declined by ~50%, suggesting partial restoration of the calcium influx pathway. A similar observation was obtained by measuring Na^+/K^+ATPase activity, which was markedly reduced in SLOS cells compared with control cells (Fig. 5). Moreover, like calcium permeability, partial restoration of membrane Na^+/K^+ATPase activity was observed in SLOS cells after cholesterol enrichment. That these data reflect membrane function specifically at the cell's plasma membrane is implied because the measurements were made using ion translocation ($^{45}Ca^{2+}$ and ^{86}Rb, extracellular to intracellular) in cell monolayers as well as the activity of a protein asymmetrically distributed to the cell surface membrane (Na^+/K^+ATPase).

Another plasma membrane protein whose activity we assessed is the folate transport protein. Folate uptake into SLOS cells was depressed by ~50% compared with control cells. Because cleft palate is well known to result, in part, from folate deficiency in the general population, and cleft palate malformations occur in 40–50% of SLOS children (41), we suggest that impaired folate uptake across the cell membrane may lead to intracellular folate deficiency and thereby contribute to the common appearance of cleft palate in SLOS. The precise location of the folate uptake pathway in the plasma membrane has not been established, but recent studies localize it to cholesterol-rich membrane domains of either the caveolar (42) or noncaveolar (43) lipid raft types.

The final membrane-mediated activity we investigated was the generation of signaling IPs. These second messengers, particularly IP_3, are involved in regulating intracellular calcium levels in response to a variety of extracellular stimuli. We observed essentially uniform reductions in IP_1, IP_2, IP_3, and total IP levels in SLOS cells compared with control cells. This impairment in IP signaling raises the question of impaired cell signaling by the IP pathway. One of the important cell functions regulated by IP signaling is cell calcium modulation and its control over cell proliferation (44, 45). As shown in Fig. 8, cell proliferation, based on [^{3}H]thymidine incorporation into cellular DNA, is significantly suppressed in SLOS cells compared with control cells. Although the cellular basis for this effect cannot be established from our data, its suppression in SLOS cells is consistent with impaired IP_3 signaling. The relevance of these observations to SLOS may be important because SLOS patients almost uniformly demonstrate a failure to grow normally, and a generalized impairment in cell proliferation may contribute to impaired somatic growth and/or development.

Relevant to our findings are those reported by Wassif et al. (46), who created a DHCR7 null mouse model of SLOS that has many of the same malformations and neurologic abnormalities seen in human SLOS. They demonstrated marked impairment of glutamate-activated Na^+ currents in cortical neurons from these animals. Importantly, this impaired activity did not appear to be caused by alterations in glutamate receptor subunit mRNA expression determined by RT-PCR, consistent with our proposal that the cell membrane may be altered in SLOS in ways that interfere with receptor activity. Interestingly, these same experiments failed to show differences in voltage-activated, tetrodotoxin-sensitive, or γ-aminobutyrate-activated Na^+ currents between control and SLOS animals, indicating a selective effect of SLOS on glutamate receptor-mediated activity.

The current study focuses specifically on the potential for abnormal sterol composition of the cell membrane to induce a generalized membrane defect in SLOS. We show that two specific membrane-mediated abnormalities, cell calcium permeability and Na^+/K^+ATPase activity, occur in SLOS fibroblasts. Because restoring membrane cholesterol content without altering the 7-DHC accumulation in SLOS cells resulted in only partial restoration of activity, we postulate that the defect is not mediated by a reduction in membrane cholesterol content alone but rather by the combination of reduced cholesterol plus the accumulation of 7-DHC in the membrane. Although we report on plasma membrane structure/function in this study, it should be noted that similar alterations may occur in intracellular membranes as well (e.g., endoplasmic reticulum,

Golgi, etc.). Unfortunately, however, treatment of SLOS patients with cholesterol-supplemented diets has demonstrated only minor amelioration of symptoms (22, 47–50), including improvements in growth and behavior (5). A limiting factor with dietary treatment is that much of the damage may occur very early during critical periods in fetal developmental. However, treatment with cholesterol-rich diets may have a greater benefit when given to infants than when initiated later in life, although improvement has been documented in adults with this dietary approach (50). In adult rats treated with BM 15.766, Xu et al. (21) have shown that cholesterol feeding fully restores plasma cholesterol levels and reduces plasma 7-DHC levels by ~50%. Further improvements were seen when the feeding protocol included cholic acid to improve hepatic bile formation or lovastatin to induce the upregulation of cell surface LDL levels.

Just how the altered sterol composition of the cell membrane mediates the changes in membrane function cannot be fully elucidated from this study. On the one hand, a homogeneous alteration in membrane viscosity can be seen to hinder and/or distort the activity of membrane proteins, leading to the changes we (28) and others (51) have observed previously. However, membranes are known to be heterogeneous structures with discrete membrane domains. In particular, both raft and caveolar domains are rich in cholesterol and highly dependent on this sterol for function. It is particularly noteworthy that all of the altered membrane-mediated functions observed in this study are known to be associated with either rafts or caveolae. Caveolae are cholesterol-rich domains containing the scaffolding protein caveolin, the signature protein of caveolae. They occur in a variety of cells, including cardiovascular and neural cells, and are abundant in fibroblasts. Importantly, caveolae appear to serve as signaling platforms compartmentalizing a multitude of signaling molecules, including those associated with calcium-regulating proteins, such as L-type calcium channels (52), capacitative calcium entry (52), the IP_3-like protein (53), the Na^+/K^+ATPase (37), folate uptake (42), and the phosphatidylinositol hydrolytic machinery (i.e., phospholipase C) (54). Likewise, glutamate receptors have been localized to caveolae, as shown by Burgueno et al. (55), which may explain the selectivity of glutamate activity observed in the SLOS mouse model. Moreover, Keller, Arnold, and Fliesler (56) have shown that although 7-DHC can combine with cholesterol, sphingomyelin, and PC to form caveolae-like bilayers, when extracted from brain tissue from rats treated with the DHCR7 inhibitor AY 9429, caveolar protein content is altered compared with that in control rat brain. Because caveolae are highly dependent on cholesterol for normal function, our data support the concept that membrane caveolar function is disturbed in SLOS.

In summary, cholesterol plays at least three major roles in cell and somatic function. First, in early embryological development, cholesterol binding to *Shh* protein is required for somatic segmentation to occur, and 7-DHC can apparently replace cholesterol without effect on *Shh* autoprocessing (23). The second role for cholesterol is in steroidogenesis, and a number of investigators have shown abnormal steroids in SLOS children that likely contribute to the SLOS phenotype (57). Third, cholesterol is essential for the synthesis of cell membranes, and it is the only sterol that mammals normally use in this capacity. In the membrane, it sets the levels of membrane fluidity, permeability, and, importantly, membrane width (24, 25, 34) appropriate for the specific membrane type (for width, plasma membrane > endoplasmic reticulum ~ Golgi > mitochondrial, etc.) (58). We show that 7-DHC cannot substitute for cholesterol in the membrane because it alters phospholipid packing and thus also membrane lipid dynamics. Because SLOS typically shows widespread organ dysfunction, we propose that the disturbance in sterol synthesis, namely the decrease in cholesterol content combined with the accumulation of 7-DHC in the membrane, accounts for the widespread abnormalities that occur in multiple organs in patients afflicted with SLOS. We further propose that membrane caveolae are particularly affected in SLOS by the abnormal sterol complement, resulting in defective cellular signaling cascades.

Support for this project was provided in part by National Institutes of Health Grants R01 HD-40284, R01 HL-66273 (T.N.T.), and R01 HL-73980 (R.D.S.) and by the Office of Research and Development, Medical Research Service, Department of Veterans Affairs (G.S.T.). The authors acknowledge Francine Hanley at Thomas Jefferson University and Yong-Feng Yang at the Oregon Health and Science University, Oregon Children's Hospital Research Center Tissue Culture Core, supported by Grant K12 HD-33703, for expert technical assistance and Jennifer Penfield for expert patient care.

REFERENCES

1. Smith, D. W., L. Lemli, and J. M. Opitz. 1964. A newly organized syndrome of multiple congenital anomalies. *J. Pediatr.* **64:** 210–217.
2. Salen, G., S. Shefer, A. Batta, G. Tint, G. Xu, A. Honda, M. Irons, and E. Elias. 1996. Abnormal cholesterol biosynthesis in the Smith-Lemli-Opitz syndrome. *J. Lipid Res.* **37:** 1169–1180.
3. Steiner, R., L. Martin, and R. Hume. 1999. Smith Lemli Opitz Syndrome. Emedicine Online Textbooks, St. Petersburg, FL (Accessed November 18, 2005 at http://www.emedicine.com/ped/topiclist.htm).
4. Curry, C. J., J. C. Carey, J. S. Holland, D. Chopra, R. Fineman, M. Golabi, S. Sherman, R. A. Pagon, J. Allanson, S. Shulman, et al. 1987. Smith-Lemli-Opitz syndrome type II: multiple congenital anomalies with male pseudohermaphroditism and frequent early lethality. *Am. J. Med. Genet.* **26:** 45–57.
5. Pauli, R. M., M. S. Williams, K. D. Josephson, and G. S. Tint. 1997. Smith-Lemli-Opitz syndrome: thirty-year follow-up of "S" of "RSH" syndrome. *Am. J. Med. Genet.* **68:** 260–262.
6. Wassif, C., D. Vied, M. Tsokos, W. Connor, R. Steiner, and F. Porter. 2002. Cholesterol storage defect in RSH/Smith-Lemli-Opitz syndrome fibroblasts. *Mol. Genet. Metab.* **75:** 325–334.
7. Fitzky, B., M. Witch-Baumgartner, M. Erdel, J. Lee, Y. Paik, H. Glossmann, G. Utermann, and F. Moebius. 1998. Mutations in the Δ^7-sterol reductase gene in patients with the Smith-Lemli-Opitz syndrome. *Proc. Natl. Acad. Sci. USA.* **95:** 8181–8186.
8. Waterham, H. R., F. A. Wijburg, R. C. Hennekam, P. Vreken, B. T. Poll-The, L. Dorland, M. Duran, P. E. Jira, J. A. Smeitink, R. A. Wevers, et al. 1998. Smith-Lemli-Opitz syndrome is caused by mutations in the 7-dehydrocholesterol reductase gene. *Am. J. Hum. Genet.* **63:** 329–338.

9. Wassif, C., C. Maslen, S. Kachilele-Linjewile, D. Lin, L. Linck, W. Connor, R. Steiner, and F. Porter. 1998. Mutations in the human sterol Δ^7-reductase gene at 11q12-12 cause Smith-Lemli-Opitz syndrome. *Am. J. Hum. Genet.* **63:** 55–62.
10. Lowry, R., and S. Yong. 1980. Borderline normal intelligence in the Smith-Lemli-Opitz (RSH) syndrome. *Am. J. Med. Genet.* **5:** 137–143.
11. Ryan, A., K. Bartlett, P. Clayton, S. Eaton, L. Mills, D. Donnai, R. Winter, and J. Burn. 1998. Smith-Lemli-Opitz syndrome: a variable clinical and biochemical phenotype. *J. Med. Genet.* **35:** 558–565.
12. Battaile, K., B. Battaile, L. Merkens, C. Maslen, and R. Steiner. 2001. Carrier frequency of the common mutation IVS8-1G>C in DHCR7 and estimate of the expected incidence of Smith-Lemli-Opitz syndrome. *Mol. Genet. Metab.* **72:** 67–71.
13. Nowaczyk, M., L. Nakamura, B. Eng, F. Porter, and J. Waye. 2001. Frequency and ethnic distribution of the common DHCR7 mutation in Smith-Lemli-Opitz syndrome. *Am. J. Med. Genet.* **102:** 383–386.
14. Gilbert-Barnes, E. and L. A. Barnes. 2000. The Metabolic Basis of Inherited Diseases. McGraw-Hill Book Co., New York.
15. Irons, M., E. R. Elias, G. Salen, G. S. Tint, and A. K. Batta. 1993. Defective cholesterol synthesis in Smith-Lemli-Opitz syndrome. *Lancet.* **342:** 1414.
16. Tint, G. S., M. Irons, E. R. Elias, A. K. Batta, R. Frieden, T. S. Chen, and G. Salen. 1994. Defective cholesterol biosynthesis associated with the Smith-Lemli-Opitz syndrome. *N. Engl. J. Med.* **330:** 107–113.
17. Witsch-Baumgartner, M., B. Fitzky, M. Ogorelkova, H. Kraft, F. Moebius, H. Glossmann, U. Seedorf, G. Gillessen-Kaesbach, G. Hoffmann, P. Clayton, et al. 2000. Mutational spectrum in the Delta7-sterol reductase gene and genotype-phenotype correlation in 84 patients with Smith-Lemli-Opitz syndrome. *Am. J. Hum. Genet.* **66:** 402–412.
18. Tint, G., G. Salen, A. Batta, S. Shefer, M. Irons, E. Elias, D. Abuelo, V. Johnson, M. Lambert, and R. Lutz. 1995. Correlation of severity and outcome with plasma sterol levels in variants x of the Smith-Lemli-Opitz syndrome. *J. Pediatr.* **127:** 82–87.
19. Roux, C., and M. Aubry. 1966. Action teratogene chez le rat d'un inhibiteur de la synthese du cholesterol, le AY 9944. *C. R. Soc. Biol. (Paris).* **160:** 1353–1357.
20. Roux, C., R. Dupruis, C. Horvath, and A. Giroud. 1980. Teratogenic effect of an inhibitor of cholesterol synthesis (AY 9944) in rats: correlation with maternal cholesterolemia. *J. Nutr.* **110:** 2310–2312.
21. Xu, G., G. Salen, S. Shefer, G. C. Ness, T. S. Chen, Z. Zhao, and G. S. Tint. 1995. Reproducing abnormal cholesterol biosynthesis as seen in the Smith-Lemli-Opitz syndrome by inhibiting the conversion of 7-dehydrocholesterol to cholesterol in rats. *J. Clin. Invest.* **95:** 76–81.
22. Honda, A., G. S. Tint, G. Salen, R. I. Kelley, M. Honda, A. K. Batta, T. S. Chen, and S. Shefer. 1997. Sterol concentrations in cultured Smith-Lemli-Opitz syndrome skin fibroblasts: diagnosis of a biochemically atypical case of the syndrome. *Am. J. Med. Genet.* **68:** 282–287.
23. Cooper, M., C. Wassif, P. Krakowiak, J. Taipale, R. Gong, R. Kelley, F. Porter, and P. Beachy. 2003. A defective response to Hedgehog signaling in disorders of cholesterol biosynthesis. *Nat. Genet.* **33:** 508–513.
24. Chen, M., R. P. Mason, and T. N. Tulenko. 1995. Atherosclerosis alters composition, structure and function of arterial smooth muscle plasma membranes. *Biochim. Biophys. Acta.* **1272:** 101–112.
25. Tulenko, T. N., M. Chen, P. E. Mason, and R. P. Mason. 1998. Physical effects of cholesterol on arterial smooth muscle membranes: evidence of immiscible cholesterol domains and alterations in bilayer width during atherogenesis. *J. Lipid Res.* **39:** 946–955.
26. Bligh, E. G., and W. J. Dyer. 1959. A rapid method of total lipid extraction and purification. *Can. J. Biochem.* **37:** 911–917.
27. Lowry, O. H., N. J. Rosenbrough, A. L. Farr, and R. J. Randall. 1951. Protein measurement with the Folin phenol reagent. *J. Biol. Chem.* **193:** 265–275.
28. Gleason, M. M., M. S. Medow, and T. N. Tulenko. 1991. Excess membrane cholesterol alters calcium movements, cytosolic calcium levels, and membrane fluidity in arterial smooth muscle cells. *Circ. Res.* **69:** 216–227.
29. Boesze-Battaglia, K., T. Spenser, R. J. Clayton, and R. J. Schimmel. 1996. Cholesterol redistribution within human platelet plasma membrane: evidence for a stimulus-dependent event. *Biochemistry.* **35:** 6664–6673.
30. van der Meer, B. W., R. P. van Hoeven, and W. J. van Blitterswijk. 1986. Steady-state fluorescence polarization data in membranes. Resolution into physical parameters by an extended Perrin equation for restricted rotation of fluorophores. *Biochim. Biophys. Acta.* **854:** 38–44.
31. Broderick, R., R. Bialecki, and T. N. Tulenko. 1989. Cholesterol-induced changes in rabbit arterial smooth muscle sensitivity to adrenergic stimulation. *Am. J. Physiol.* **257:** H170–H178.
32. Stevens, V., and J. Tang. 1997. Fumonisin B1-induced sphingolipiddepletion inhibits vitamin uptake via the glycosylphosphatidylinositol-anchored folate receptor. *J. Biol. Chem.* **272:** 18020–18025.
33. Carney, D. H., D. Scott, E. A. Gordon, and E. F. LaBelle. 1985. Phosphoinositides and mitogenesis: neomycin inhibits thrombin-stimulated phosphoinositide turnover and initiation of cell proliferation. *Cell.* **42:** 479–488.
34. Kahn, K., K. Battaglia, D. Stepp, A. Petrov, Y. Huang, R. Mason, and T. Tulenko. 2005. Influence of serum cholesterol on atherogenesis and intimal hyperplasia after angioplasty: inhibition by amlodipine. *Am. J. Physiol. Heart Circ. Physiol.* **288:** H591–H600.
35. Fumagalli, R., F. Bernini, G. Galli, M. Anastasia, and A. Feicchi. 1980. The identification of a novel C27 diene, cholesta-5,8-dien-3beta-ol, in tissues of rats given AY-9944 (trans-1,4-bis(2-dichlorobenzylamino-ethyl)cyclohexane) in pregnancy. *Steroids.* **35:** 665–672.
36. Rujanavech, C., P. Henderson, and D. Silbert. 1986. Influence of sterol structure on phospholipid phase behavior as detected by parinaric acid fluorescence spectroscopy. *J. Biol. Chem.* **261:** 7204–7214.
37. Rindler, M., J. McRoberts, and M. Saier. 1982. (Na^+,K^+)-cotransport in the Madin-Darby canine kidney cell line. Kinetic characterization of the interaction between Na^+ and K^+. *J. Biol. Chem.* **257:** 2254–2259.
38. Moebius, F., B. Fitzky, J. Lee, Y. Paik, and H. Glossmann. 1998. Molecular cloning and expression of the human Δ7-sterol reductase. *Proc. Natl. Acad. Sci. USA.* **95:** 1899–1902.
39. Leonard, A., and E. Dufourc. 1991. Interactions of cholesterol with the membrane lipid matrix. A solid state NMR approach. *Biochimie.* **73:** 1295–1302.
40. Yeagle, P. 1985. Cholesterol and the cell membrane. *Biochim. Biophys. Acta.* **822:** 267–287.
41. Cunniff, C., L. Kratz, A. Moser, M. Natowicz, and R. Kelley. 1997. Clinical and biochemical spectrum of patients with RSH/Smith-Lemli-Opitz syndrome and abnormal cholesterol metabolism. *Am. J. Med. Genet.* **68:** 263–269.
42. Smart, E., C. Mineo, and R. Anderson. 1996. Clustered folate receptors deliver 5-methyltetrahydrofolate to cytoplasm of MA104 cells. *J. Cell Biol.* **134:** 1169–1177.
43. Rijnboutt, S., G. Jansen, G. Posthuma, J. Hynes, J. Schornagel, and G. Strous. 1996. Endocytosis of GPI-linked membrane folate receptor-alpha. *J. Cell Biol.* **132:** 35–47.
44. Lipskaia, L., and A. Lompre. 2004. Alteration in temporal kinetics of Ca^{2+} signaling and control of growth and proliferation. *Biol. Cell.* **96:** 55–68.
45. Munaron, L., S. Antoniotti, and D. Lovisolo. 2004. Intracellular calcium signals and control of cell proliferation: how many mechanisms? *J. Cell. Mol. Med.* **8:** 161–168.
46. Wassif, C. A., P. Zhu, L. Kratz, P. A. Krakowiak, K. Battaile, F. F. Weight, A. Grinberg, R. D. Steiner, N. A. Nwokoro, R. I. Kelley, et al. 2001. Biochemical, phenotypic and neurophysiological characterization of a genetic mouse model of RSH/Smith-Lemli-Opitz syndrome. *Hum. Mol. Genet.* **10:** 555–564.
47. Sikora, D., M. Ruggiero, K. Petit-Kekel, L. Merkens, W. Connor, and R. Steiner. 2004. Cholesterol supplementation does not improve developmental progress in Smith-Lemli-Opitz syndrome. *J. Pediatr.* **144:** 783–791.
48. Nwokoro, N. A., and J. J. Mulvihill. 1997. Cholesterol and bile acid replacement therapy in children and adults with Smith-Lemli-Opitz (SLO/RSH) syndrome. *Am. J. Med. Genet.* **68:** 315–321.
49. Kelly, R. I. 1997. Editorial. A new face for an old syndrome. *Am. J. Med. Genet.* **65:** 251–256.
50. Elias, E. R., M. B. Irons, A. D. Hurley, G. S. Tint, and G. Salen. 1997. Clinical effects of cholesterol supplementation in six patients with the Smith-Lemli-Opitz syndrome (SLOS). *Am. J. Med. Genet.* **68:** 305–310.
51. Schwarz, S. M., H. E. Bostwick, and M. M. Medow. 1988. Estrogen modulates ileal basolateral membrane lipid dynamics and Na^+/K^+-ATPase activity. *Am. J. Physiol.* **254:** G687–G694.

52. Darby, P., C. Kwan, and E. Daniel. 2000. Caveolae from canine airway smooth muscle contain the necessary components for a role in Ca^{2+} handling. *Am. J. Physiol. Lung Cell. Mol. Physiol.* **279:** L1226–L1235.
53. Fujimoto, T., S. Nakade, A. Miyawaki, K. Mikoshiba, and K. Ogawa. 1992. Localization of inositol 1,4,5-trisphosphate receptor-like protein in plasmalemmal caveolae. *J. Cell Biol.* **119:** 1507–1513.
54. Jang, I., J. Kim, B. Lee, S. Bae, M. Park, P. Suh, and S. Ryu. 2001. Localization of phospholipase C-gamma1 signaling in caveolae: importance in EGF-induced phosphoinositide hydrolysis but not in tyrosine phosphorylation. *FEBS Lett.* **491:** 4–8.
55. Burgueno, J., C. Enrich, E. Canela, J. Mallol, C. Lluis, R. Franco, and F. Ciruela. 2003. Metabotropic glutamate type 1alpha receptor localizes in low-density caveolin-rich plasma membrane fractions. *J. Neurochem.* **86:** 785–791.
56. Keller, R., T. Arnold, and S. Fliesler. 2004. Formation of 7-dehydrocholesterol-containing membrane rafts in vitro and in vivo, with relevance to the Smith-Lemli-Opitz syndrome. *J. Lipid Res.* **45:** 347–355.
57. Shackleton, C., E. Roitman, L. Guo, W. Wilson, and F. Porter. 2002. Identification of 7(8) and 8(9) unsaturated adrenal steroid metabolites produced by patients with 7-dehydrosterol-delta7-reductase deficiency (Smith-Lemli-Opitz syndrome). *J. Steroid Biochem. Mol. Biol.* **82:** 225–232.
58. Bretscher, M., and S. Munro. 1993. Cholesterol and the Golgi apparatus. *Science.* **261:** 1280–1281.